Reciprocal effect on lateral diffusion of receptor for advanced glycation endproducts and toll-like receptor 4 in the HEK293 cell membrane

<sup>1</sup>Mohammad Khalid Ibne Walid, <sup>1</sup>Sharifur Rahman, Emily A. Smith\*

<sup>1</sup>These authors have contributed equally to the work.

Department of Chemistry, Iowa State University, Ames, IA, 50011, United States

\*Corresponding author: esmith1@iastate.edu

ORCID ID: 0000-0001-7438-7808

**Abstract** 

Receptor for advanced glycation endproducts (RAGE) and toll-like receptor 4 (TLR4) are pattern-

recognition receptors that bind to molecular patterns associated with pathogens, stress, and cellular

damage. Diffusion plays an important role in receptor functionality in the cell membrane.

However, there has been no prior investigation of the reciprocal effect of RAGE and TLR4

diffusion properties in the presence and absence of each receptor. This study reports how RAGE

and TLR4 affect the mobility of each other in the human embryonic kidney (HEK) 293 cell

membrane. Diffusion properties were measured using single particle tracking (SPT) with quantum

dots (QDs) that are selectively attached to RAGE or TLR4. The Brownian diffusion coefficients

of RAGE and TLR4 are affected by the presence of the other receptor, leading to similar diffusion

coefficients when both receptors coexist in the cell. When TLR4 is present, the average Brownian

diffusion coefficient of RAGE increases by 40%, while the presence of RAGE decreases the

average Brownian diffusion coefficient of TLR4 by 32%. Diffusion in confined membrane

domains is not altered by the presence of the other receptor. The mobility of the cell membrane

lipid remains constant whether one or both receptors are present. Overall, this work shows that the

presence of each receptor can affect a subset of diffusion properties of the other receptor without

affecting the mobility of the membrane.

Keywords Single-particle tracking, receptor dynamics, live cell imaging, fluorescence

microscopy, receptor cross talk

1

## **Abbreviations**

**AHA** Antibody to HA epitope

Amyc Antibody to myc epitope

**ANOVA** Analysis of variance

**CD14** Cluster of differentiation 14

EDTA Ethylene diamine tetra acetic acid

HEK293 Human embryonic kidney 293 cells

**HA** Hemagglutinin

MD2 Myeloid differentiation protein 2

**QDs** Quantum dots

**RAGE** Receptor for advanced glycation endproducts

**SPT** Single Particle Tracking

TLR4 Toll-like receptor 4

#### Introduction

Biological membranes exhibit dynamic attributes crucial to multiple cellular processes, such as signal transduction, cell adhesion, and molecular transport (Schopf & Huber, 2017). Integral to membrane function, receptors facilitate diverse cellular functions, including ion transport, receptor signaling, and enzymatic activity (Nozeret et al., 2019; Syed et al., 2018; Trofimov et al., 2019). The location and abundance of membrane proteins are crucial for their specific roles within cells, and the mobility of receptors within the cell membrane is needed for their proper functioning. The ability to move allows intercellular communication, sensing external environments, endocytosis, and signal generation (Bian et al., 2012; Lazar et al., 2020; Semini et al., 2017).

The receptor for advanced glycation endproducts (RAGE) is a member of the immunoglobulin superfamily of cell surface molecules, and toll-like receptor 4 (TLR4) is one of the ten members of the toll-like receptor family in humans. Both are pattern recognition receptors that can detect and respond to pathogen-associated molecular patterns and damage-associated molecular patterns (Areal et al., 2011; Syed et al., 2018; Zhong et al., 2020). RAGE and TLR4 are critical for immune responses and inflammatory signaling pathways (Casula et al., 2011). RAGE is expressed in different types of cells like monocytes/macrophages, granulocytes, adipocytes, vascular smooth muscle, and some cancer cells, while TLR4 is primarily expressed in immune cells like monocytes, macrophages, dendritic cells, B cells, and neutrophils (Goldin et al., 2006a; McGettrick & O'Neill, 2007; Płóciennikowska et al., 2015). RAGE and TLR4 are transmembrane proteins with an extracellular domain, transmembrane domain, and cytoplasmic tail (Kim et al., 2013; Syed et al., 2018). The RAGE extracellular domain has one variable-type domain and two constant-type domains (i.e., C1 and C2) (Syed et al., 2018). With these three domains, RAGE can recognize and bind with many different ligands. On the other hand, TLR4 needs two coreceptors, myeloid differentiation protein 2 (MD2) and cluster of differentiation 14 (CD14), to recognize and bind ligands (Kim et al., 2013).

The function of RAGE and TLR4 is linked during inflammatory responses (Sakaguchi et al., 2011; Yan et al., 2023). Both receptors share some common ligands, including advanced glycation endproducts, high mobility group box 1 protein, and S100 proteins, and have common inflammatory signaling pathways (Gąsiorowski et al., 2018; Ibrahim et al., 2013; Lin, 2006). Previously, fluorescence resonance energy transfer and direct stochastic optical reconstruction

microscopy were used to visualize the clustering of RAGE and TLR4 on cell membrane. These studies show that both proteins have nanoscale structures on cell membrane (Xie et al., 2008; Zeuner et al., 2016). Besides some functional similarities, RAGE and TLR4 activation results in the convergence of synergistic shared downstream signaling pathways, known as "crosstalk" (Ibrahim et al., 2013; Van Beijnum et al., 2008). Previous studies suggest that the signal transduction crosstalk between RAGE and TLR4 might result from their physical interaction on the cell membrane, causing enhanced inflammation (Prantner et al., 2020). Although the signal transduction crosstalk between RAGE and TLR4 has been studied for the last two decades, how each receptor affects the other's diffusional properties remains unknown (Prantner et al., 2020; Yan et al., 2023; Zhong et al., 2020). The diffusion of receptors could be affected by multiple factors, and interactions with other proteins are expected to be prominent (Maynard & Triller, 2019). Furthermore, RAGE and TLR4 are promising therapeutic targets for many inflammation-related diseases (Prantner et al., 2020). To have a complete understanding of the function of these receptors, it is imperative to know how these receptors diffuse on the cell membrane.

There are many techniques to measure the diffusion of receptor proteins on cell membrane. Fluorescence recovery after photobleaching is one of the most widely used techniques for measuring protein diffusion on cell membrane, but fluorescence recovery after photobleaching provides the diffusion properties averaged over tens, hundreds, or thousands of receptors (e.g., the average of many RAGE receptors). It is an ensemble technique. Receptor diffusion is heterogeneous, and many diffusion behaviors are often observed for the same receptor. To measure this heterogeneity, that is to measure the different populations, it is imperative to track receptors individually. Single particle tracking (SPT) has been utilized to study the diffusion of individual proteins and the heterogeneity in their diffusion properties in live cells. For example, SPT has been used to measure the confined diffusion coefficients of RAGE in bovine artery GM07373 endothelial cells after treating the cells with methylglyoxal-modified bovine-serum-albumin ligand; the confined diffusion properties of RAGE change after ligand treatment (Syed et al., 2016). Rouiller et al. (2009) used two-color SPT experiments, where two different quantum dots are simultaneously tracked using their unique optical signals, to simultaneously track two different proteins on the same cell (Rouiller et al., 2009). These experiments provide information about how one receptor affects the diffusion properties of the other receptor. Herein, we utilized SPT and twocolor SPT to study the diffusional properties of RAGE and TLR4 on the cell membrane of human

embryonic kidney (HEK) 293 cells to shed light on possible synergistic effects of RAGE diffusion and TLR4 diffusion.

#### Materials and methods

### Cell culture

All the experiments used HEK293 cells from American Type Culture Collection: CRL-1573. Cells were cultured in Dulbecco's modified eagle's medium (Sigma Aldrich) with 10% fetal bovine serum, 36.5 mM penicillin, and 12.5 mM streptomycin (Fisher Scientific) and incubated in a humidified incubator (ThermoScientific) with 5% CO<sub>2</sub> at 37 °C. Cells were sub-cultured every two or three days using a 0.25% (w/v) trypsin-EDTA solution (Life Technologies).

# HA-RAGE, MD2/CD14 and myc-TLR4 plasmid transfection

The cells used in this study were transfected to express hemagglutinin (HA)-epitope-tagged RAGE (HA-RAGE), myc-epitope-tagged TLR4 (myc-TLR4), MD2, and CD14 proteins. Hemagglutinin (HA) tags, which have the nine amino acid sequence YPYDVPDYA, and myc tags, which have the ten amino acid sequence EQKLISEEDL, were added to the extracellular domains of RAGE and TLR4, respectively, so that antibody-conjugated quantum dots can bind specifically to the receptors. The notation for the cell lines used throughout the text is shown in Table 1. Details of the expression plasmid of HA-RAGE and its transfection were described earlier (Syed et al., 2016). A plasmid containing the gene sequences for human MD2 and CD14, pDUO2-hMD2/CD14, was purchased from InvivoGen and transformed into DH5α E. coli cells. Transformed cells were grown and selected on Petri dishes containing 200 ml of E. coli Fast-Media® Hygro (InvivoGen). HEK293 (-) cells and HEK293 RAGE (-) were transfected with purified pDUO2-hMD2/CD14 plasmid using Lipofectamine 3000 following the manufacturer's instructions (Invitrogen<sup>TM</sup>) to generate HEK293 (+) and HEK293 RAGE (+) after selection using 200 µg/ml Hygromycin B in the DMEM complete medium. A plasmid for expressing myc epitope at the N-terminal of TLR4, pcMV3-puro-mycTLR4, was obtained from Sino Biological, China. Competent NEB 5α E. coli cells were employed for plasmid expression, and transformed cells were grown and selected on Miller's LB Agar (US Biological, Life Sciences) containing 100 µg/ml Ampicillin (Fisher BioReagents<sup>TM</sup>). Purified pcMV3-puro-mycTLR4 plasmid was used to transfect HEK293 (-) cells,

HEK293 (+) cells, HEK293 RAGE (-) cells and HEK293 RAGE (+) cells. The transfection was performed using Lipofectamine 3000, following the manufacturer's instructions (Invitrogen<sup>TM</sup>) to generate HEK293 TLR4 (-), HEK293 TLR4 (+), HEK293 RAGE TLR4 (-) and HEK293 RAGE TLR4 (+) after selection using 0.5 μg/ml puromycin in the Dulbecco's modified eagle's complete medium.

Table 1. Notations for all the transfected HEK293 cell lines

<b>Expressing</b> HA	Expressing myc	Expressing	Cell notation
epitope-tagged RAGE	epitope-tagged TLR4	MD2 CD14	
		(+)	
			HEK (-)
		✓	HEK (+)
✓			HEK RAGE (-)
✓		✓	HEK RAGE (+)
	✓		HEK TLR4 (-)
	✓	✓	HEK TLR4 (+)
✓	✓		HEK RAGE TLR4 (-)
✓	✓	✓	HEK RAGE TLR4 (+)

## Antibody-quantum dot (QD) preparation

Streptavidin-coated QDs were used throughout this study. Biotinylated monoclonal HA-epitopetag antibody (AHA) was coated on the QD (AHA-QDs) to label HA-RAGE for SPT experiments as described by Syed et al. (2016). The same procedure was followed to prepare monoclonal mycepitope-tag antibody (Amyc, ThermoFisher Scientific) QDs (Amyc-QDs) to label myc-TLR4. For the single-color SPT experiments, QD605 (ThermoFisher Scientific) was used. For the two-color SPT experiments, QD585 (ThermoFisher Scientific) and QD655 (ThermoFisher Scientific) were used to label HA-RAGE and myc-TLR4, respectively, in the same cell.

## Cell sample preparation for the SPT experiments

For SPT experiments, Nunc<sup>TM</sup> Lab-Tek<sup>TM</sup> chambered glass slides with 8 wells were pre-treated with a sterile solution of 0.01% poly-L-lysine (Sigma Aldrich) for 15 minutes, washed with deionized water and then air dried. Cells were grown onto these slides for 48 hours, then the culture medium was discarded, and cells were incubated with Dulbecco's modified eagle's medium containing 3% (w/v) bovine serum albumin for 18 hours to cover the areas of the glass slide that do not have any cells to reduce nonspecific binding. Immediately before performing SPT experiments, the medium was replaced by the appropriate antibody-QD solution diluted in HEPES imaging buffer containing 0.1% bovine serum albumin for 15 minutes at 37 °C and rinsed with HEPES imaging buffer several times prior to performing the microscopy experiments. A 100 pM AHA-QD or Amyc-QD solution was used for SPT experiments. For the two-color SPT experiments, 50 pM of AHA-QD and 50 pM Amyc-QD solutions were used concurrently.

## **SPT** experiment

SPT experiments were performed using a Nikon Eclipse TE2000U microscope with a  $100 \times 1.49$  numerical-aperture oil-immersion objective. The microscope was operated in epi-fluorescence, wide-field mode surrounded by a  $37 \pm 2$  °C home-built thermal chamber. Light from a mercury lamp (X-Cite 120 PC) was filtered using a 370/35 nm (central wavelength passed/width of the passed band of wavelengths) bandpass filter to excite the sample, and emitted light was filtered using a 605/20 nm bandpass filter. An Andor iXon EM+DU-897 back-illuminated electron-multiplying charge-coupled device was used to collect the emitted light with an acquisition time of 40 ms per frame, and 1000 frames per data were collected. To monitor the movement of QDs, a sequence of images is collected at regular time intervals to create a dataset analogous to a movie. Each individual image within the movie is a "frame," and within these frames the QDs appear as discrete points. Tracking these discrete points across all the frames generates a trajectory that shows the QD's travel over time. At least 102 mobile trajectories of AHA-QDs or Amyc-QDs from at least 15 cells were measured for each data set. The spatial uncertainty was 17 nm for all SPT experiments.

### **Two-color SPT experiment**

To track both RAGE and TLR4 proteins in the same cell, a dual-view imager (Optical Insight, LLC) was placed between the microscope and the detector to separate the emission from QD585 and QD655. Emission light from QD585 was filtered into channel 1 on the left side of the image

using a 605/52 nm filter, and emission light from QD655 was filtered into channel 2 on the right side of the image using a 635/20 nm filter. As described above, the SPT experiments used a 40 ms collection time, which isolated the QD signal into two channels. However, using a 1 s collection time, signal from both QDs could be detected in channel 1. Comparing the images collected at 40 ms and 1 s for the same sample allowed the two QD populations to be identified, and this acted as a fiducial marker to spatially align the channel 1 and channel 2 images. Other experimental parameters were the same as described in the section above (SPT experiment).

### **Data analysis**

For detecting and localizing the signal from the QDs, the ImageJ-based plugin "2D/3D particle tracker" was used to track the particle movement and generate trajectories (Mainali & Smith, 2013a; Sbalzarini & Koumoutsakos, 2005). While producing the trajectory of a detected and localized particle at a frame, three consecutive frames were needed to link the particles into a trajectory. A maximum of four pixels were allowed for the displacement of a particle between two consecutive frames. Each pixel represents a 160 nm distance. To analyze the movement of the particles, trajectory data was analyzed using a MATLAB-based application named "Analyzing Particle Movement with Graphical User Interface" (Menchón et al., 2012; Simson et al., 1995).

# Statistical analysis

Statistical significance between the datasets was determined using a one-way analysis of variance (ANOVA) followed by the F-test using JMP software. The difference between the two data sets was deemed significant when the estimated probability (p) value was less than 0.05.

# Immunofluorescence of HA tag, myc tag, and CD14 protein

Cells were grown in Nunc<sup>TM</sup> Lab-Tek<sup>TM</sup> chambered glass slides with 8 wells, which were pretreated with a sterile 0.01% poly-L-lysine (Sigma Aldrich) solution for 15 minutes and then washed with deionized water and air dried. To fix the cell membrane, 1% paraformaldehyde solution in phosphate buffered saline was used to incubate the cells for 10 minutes at room temperature. Cells were washed with phosphate buffered saline solution and incubated in the incubation buffer (5% normal goat serum and 1% bovine serum albumin in phosphate buffered saline) for 30 minutes at room temperature. Then, the cells were incubated with the appropriate primary antibody diluted in incubation buffer at room temperature for 1 hour. This study employed monoclonal primary

antibodies. The antibodies were anti-HA tag (Invitrogen<sup>TM</sup>) at a dilution of 1:500, anti-RAGE (Santa Cruz Biotechnology) at a dilution of 1:200, anti-myc tag (ThermoScientific) at a dilution of 1:100, anti-TLR4 (ThermoScientific) at a dilution of 1:200, and anti-CD14 (Santa Cruz Biotechnology) at a dilution of 1:200. The secondary antibody was polyclonal goat anti-mouse Alexa Fluor<sup>TM</sup> plus 647. Cells were incubated with secondary antibody at room temperature for 30 minutes. Finally, the cells were washed three times with phosphate buffered saline and imaged in the same buffer.

#### Results and discussion

## Expression of HA-RAGE, myc-TLR4, and CD14 proteins in the transfected cell lines

The HEK293 cells used in this work were transfected to express HA-RAGE, myc-TLR4, MD2, and/or CD14 proteins, and the expression of these proteins in the cell membrane was confirmed using immunofluorescence experiments. MD2 and CD14 are two coreceptors for TLR4 that are required for ligand binding (Kim et al., 2013). Immunofluorescence images showed distinct localization patterns at the edge of the cell for HA-RAGE (Fig. 1a and Fig. 2a), myc-TLR4 (Fig. 1b and Fig. 2b), and CD14 (Fig. 3) in cell lines that were transfected to express these proteins. This localization pattern of the cell membrane proteins aligns with previous studies (Manzoni et al., 2004; Wang et al., 2008). In contrast, cells that were not transfected show no binding of the HA-RAGE (Fig. 1a and Fig. 2a), myc-TLR4 (Fig. 1b and Fig. 2b), and CD14 (Fig. 3) antibodies and no detectable endogenous expression. MD2 is excreted from the cell (Chen et al., 2020) and could not be detected by immunofluorescence (data not shown).

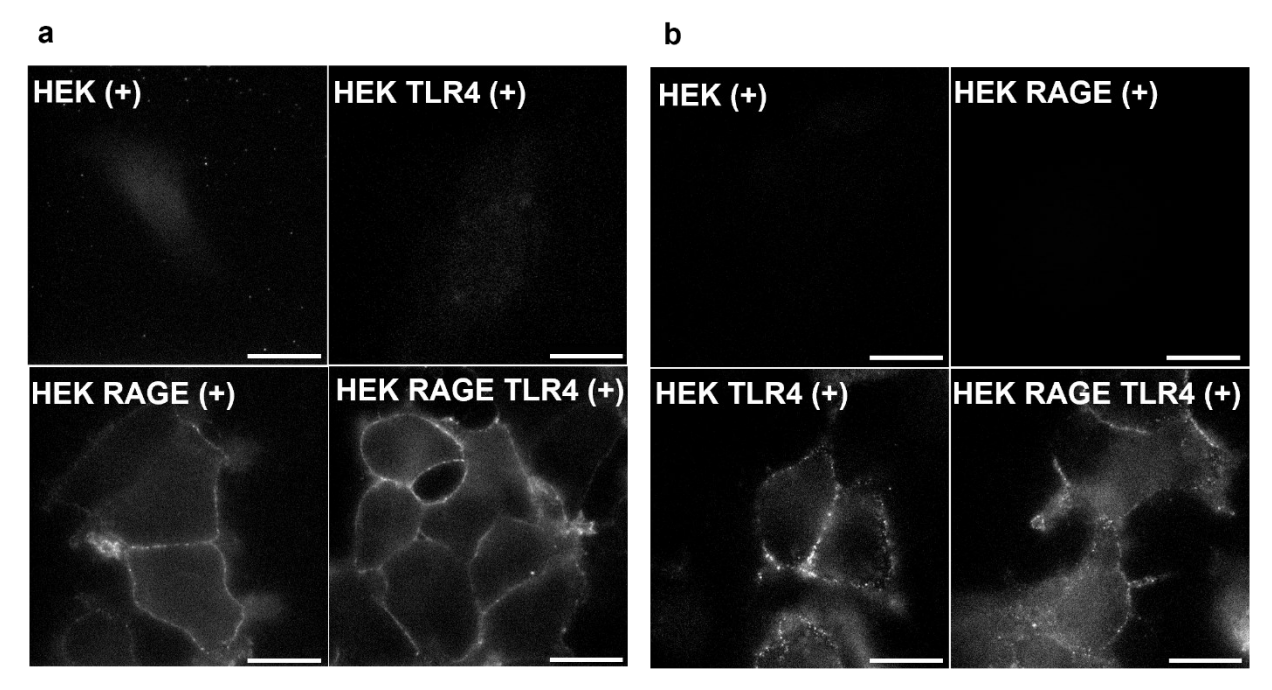


**Fig. 1** Immunofluorescence images with (a) HA primary antibody and (b) myc primary antibody in the indicated HEK293 cell line. The upper row of images shows the control data in cells that lack expression of the target protein (a) lacking HA-tagged RAGE, (b) lacking myc-tagged TLR4. The lower row of images in **a** shows the signal from HA-tagged RAGE. The lower row of images in **b** shows the signal from myc-tagged TLR4. The spatial scale bar is 20 μm in all the images. All images are shown in the same intensity scale

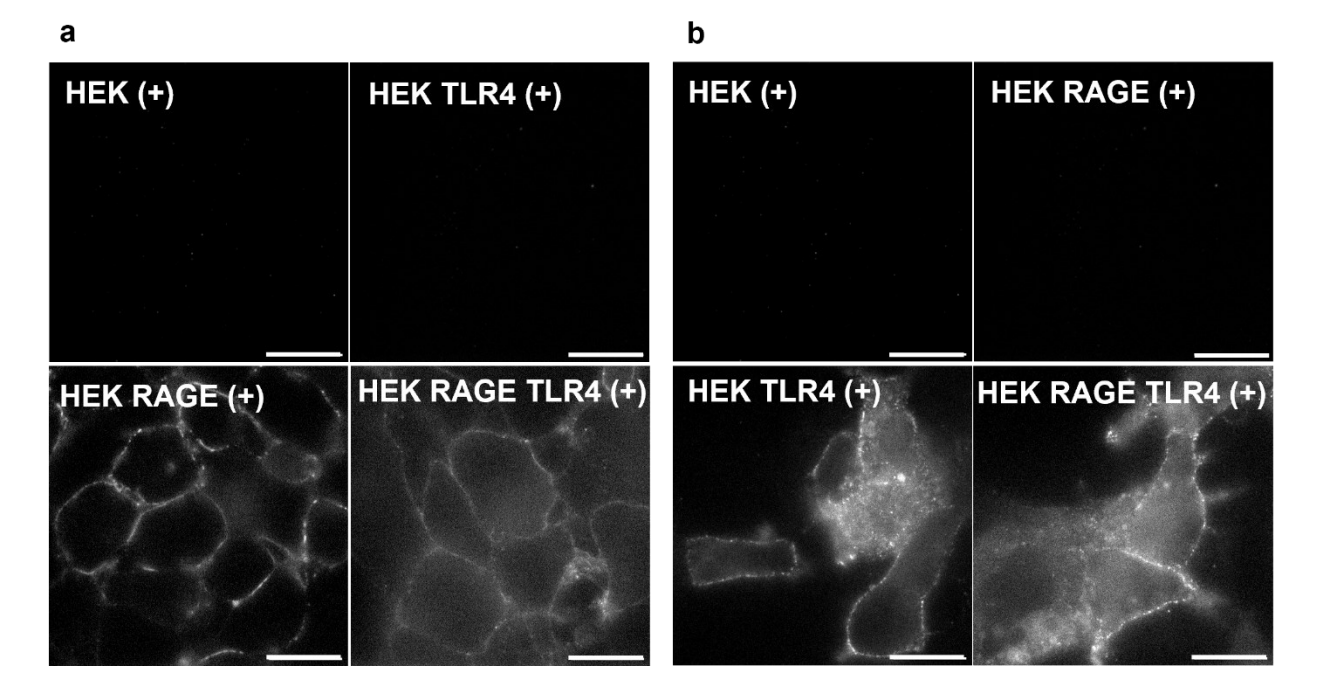


**Fig. 2** Immunofluorescence images with (a) RAGE primary antibody and (b) TLR4 primary antibody on the membrane of the indicated HEK293 cell line. The upper row of images shows the control data in cells that lack expression of the target protein (a) lacking HA-tagged RAGE and (b) lacking myc-tagged TLR4. The lower row of images in **a** shows signal from HA-tagged RAGE. The lower row of images in **b** shows signal from myc-tagged TLR4. The spatial scale bar is 20 μm in all the images. All images are shown in the same intensity scale

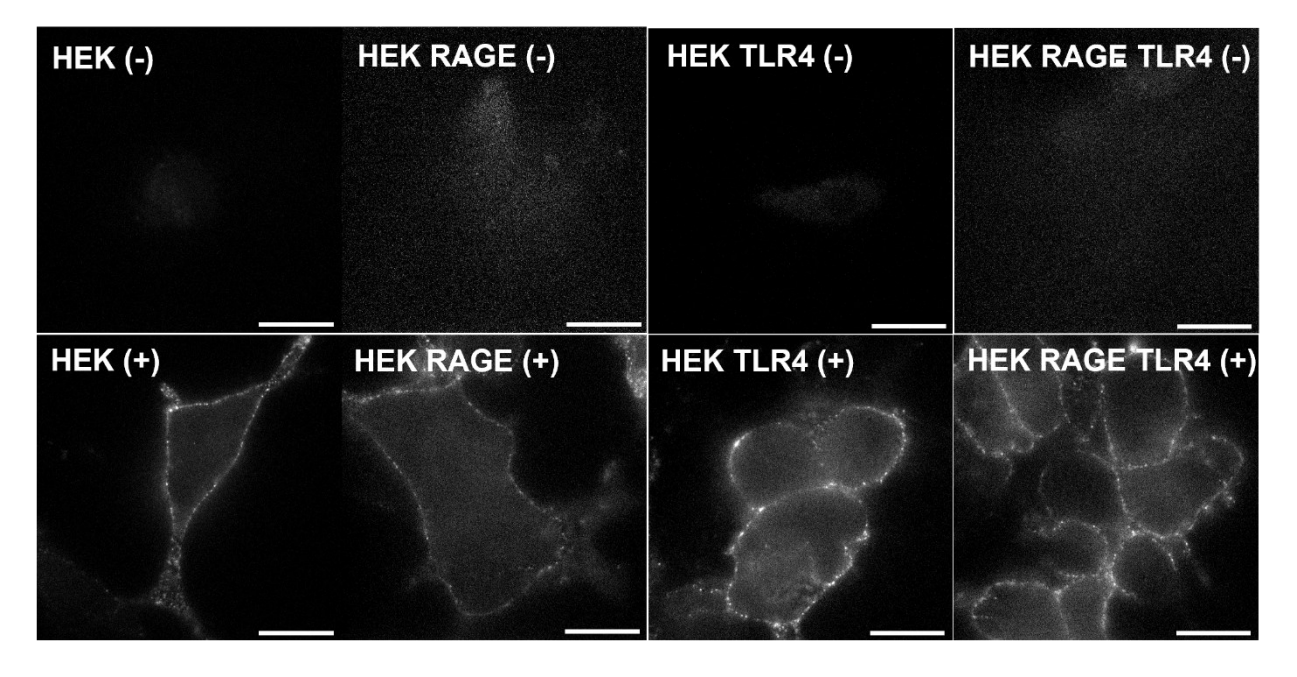


**Fig. 3** Immunofluorescence images of CD14 on the membrane of the indicated HEK293 cell line. The upper row of images shows the control data in cells that lack expression of CD14. The lower row of images shows the signal from CD14 in cells that have been transfected to express CD14. The spatial scale bar is 20 μm in all the images. All images are shown in the same intensity scale

# Extracellular HA and myc epitope tags facilitate the specific labeling of QDs to RAGE and TLR4, respectively

The successful implementation of SPT experiments relies on the specific binding between a QD and a receptor. Under these conditions, the movement of the QD reflects the movement of the receptor. The movement is reflected in a trajectory, which is the reconstruction of the path traversed by the QDs as measured in the series of luminescence images (i.e., movie). The trajectory encodes valuable information regarding the diffusion properties of the receptor responsible for generating it. Directly coating the surface of the QDs with RAGE ligands like S100A8/A9 or advanced glycation endproducts results in a large amount of nonspecific binding to the cell (Mainali & Smith, 2013b; Michalet et al., 2005). This nonspecific binding is attributed, in part, to the ligands binding to receptors other than RAGE (Goldin et al., 2006a). To reduce nonspecific binding and obtain useful SPT trajectories, it is necessary to use extracellular HA and myc epitope tags on

RAGE and TLR4, respectively. The QDs are coated with antibody to HA (AHA) or antibody to myc (Amyc) to generate AHA-QDs and Amyc-QDs.

Table 2. Percent nonspecific binding of the AHA-QDs and Amyc-QDs on the cell lines

Antibody-	Cell line to test	Number	Control cell	Number of	Nonspecific
quantum	specific binding	of	line to test	quantum	Binding
dot (QD)		quantum	nonspecific	dots per	(%)
		dots per	binding	cell for	
		cell for		nonspecific	
		specific		binding <sup>1</sup>	
		binding <sup>1</sup>			
AHA-QDs	HEK RAGE (+)	11.82	HEK (+)	0.25	2
Amyc-QDs	HEK TLR4 (+)	29.88	HEK (+)	0.16	1
AHA-QDs	HEK RAGE TLR4	13.32	HEK TLR4 (+)	0.55	4
	(+)				
Amyc-QDs	HEK RAGE TLR4	8.52	HEKRAGE (+)	0.29	3
	(+)				

<sup>1</sup> The quantification per cell is performed on a minimum of 50 cells.

The extent to which AHA-QDs or Amyc-QDs bind specifically to their targeted receptor was measured with control experiments performed in cells lacking the expression of RAGE and TLR4 as well as cells that expressed the receptors (Table 2). The nonspecific binding was calculated by counting the average number of QDs per cell lacking receptor and the average number of QDs per cell expressing receptor. The nonspecific binding observed for AHA-QD and Amyc-QD was within the 1-4% range (Table 2). This low level of nonspecific binding is consistent with other successful SPT experiments (Syed et al., 2016).

It has been previously reported that the trajectories measured in cells lacking receptor expression show no movement (i.e., the nonspecific binding results in immobile trajectories) (Goldin et al., 2006b). The diffusion coefficient for the trajectories measured in HEK293 cells lacking receptor expression is  $0.0018 \, \mu m^2/s$  (Zhu & Smith, 2019a). To ensure the accuracy of reported RAGE or

TLR4 diffusion data, all trajectories with a diffusion coefficient below  $0.0018~\mu m^2/s$  were excluded from the analysis discussed below. The exclusion of the immobile trajectories poses a limitation in accurately quantifying the proportion of immobile RAGE and TLR4 in the cell membrane. On the other hand, excluding these trajectories prevents biasing the diffusion properties with results from nonspecific binding.

# Confined diffusion properties of RAGE and TLR4 are not affected by the presence of the other receptor

The mobile trajectories showed two types of diffusion: Brownian and confined. Confined diffusion is classified based on criteria that has been previously reported (Simson et al., 1995). A confined domain is a region in the cell membrane where receptors remain for a period longer than can be modeled by Brownian diffusion. Outside of confined domains, the diffusion is Brownian.

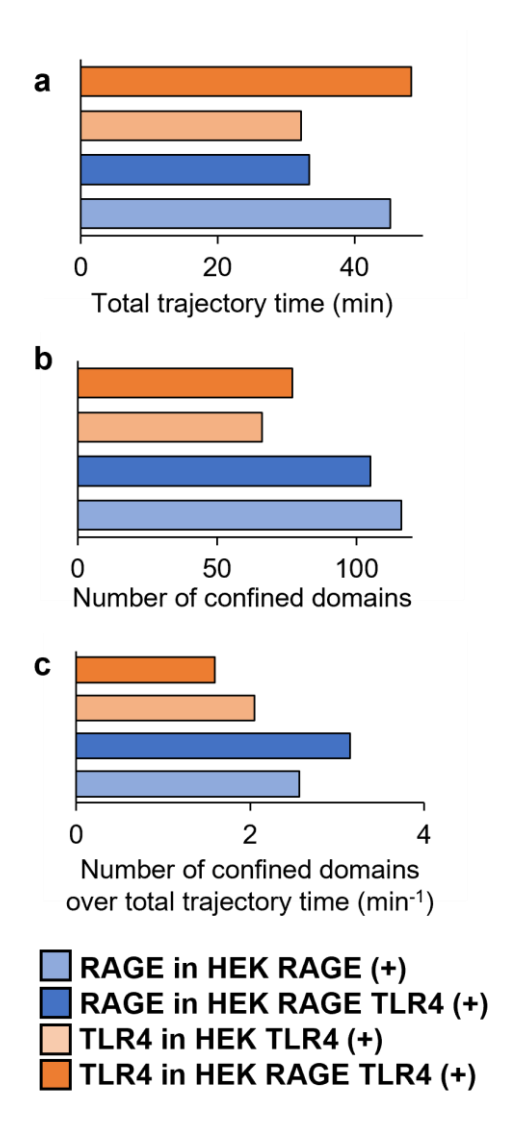


**Fig. 4** Characteristics of the trajectories of (blue) RAGE and (orange) TLR4. **a** shows the sum of the duration of each trajectory in the data set (total trajectory time), **b** shows the sum of all confined domains measured in all trajectories for the data set, and **c** shows the number of confined domains detected per minute of the total trajectory time. These values are obtained by counting total events, so no error bars are presented

The segments of the trajectories when the receptor is displaying non-Brownian diffusion were assessed to analyze confined diffusion properties. There are many possible reasons a receptor may transiently exhibit non-Brownian diffusion, including macromolecular crowding, compartmentalization into heterogeneous domains, and protein binding to the cytoskeleton, etc. (Gambin et al., 2006; Syed et al., 2018).

For all cell lines, the luminescence movies were collected for approximately 35-40 minutes. However, a different number of trajectories are recorded over this measurement time for each cell line. This is primarily due to the varying number of QDs bound to the cells, the varying number of cells in the image, and the QD's intrinsic blinking, which results in a temporary turn-off of the QD's luminescence (Syed et al., 2016). Also, not all QDs can be tracked due to requirements in constructing the trajectories (Sbalzarini & Koumoutsakos, 2005). For these reasons, the total trajectory time (Fig. 4a) and the number of trajectories measured for each cell line (Fig. 4b) were different. To avoid biasing the number of measured confined diffusion events, the number of times the receptor was measured in a confined domain was normalized to the total trajectory time (Fig. 4c). Fig. 4c shows that RAGE enters approximately 2.6 (without TLR4 expression) to 3.2 (with TLR4 expression) confined domains per minute while TLR4 enters approximately 1.6 (with RAGE expression) to 2.0 (without RAGE expression) confined domains per minute. RAGE enters into more confined domains per minute compared to TLR4, and this is true whether TLR4 is present or not present in the membrane.

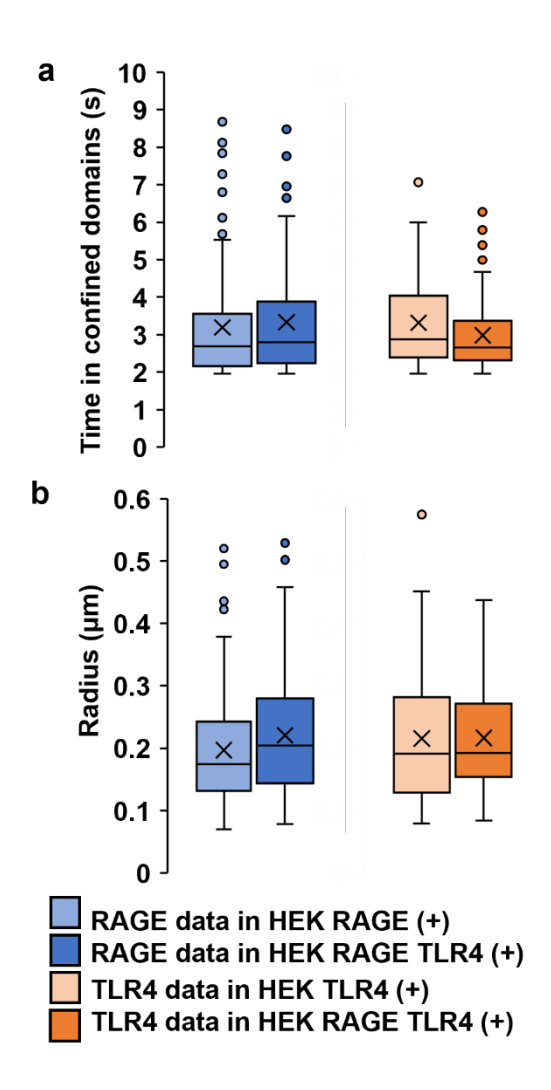


**Fig. 5** The box-and-whisker plots showing diffusion properties within the confined domain for (blue) RAGE and (orange) TLR4. **a)** the receptor's time in a confined domain (confinement time) and **b)** the radius of the confined domain. All comparisons result in a p-value above 0.05 and are not statistically significant

When a receptor enters a confined domain, the amount of time it exhibits confined diffusion before once again exhibiting Brownian diffusion is measured (time in confined domain) as well as the size of the confined domain (radius of confinement). The average time in confined domains for RAGE in the absence and presence of TLR4 is 3.2 seconds and 3.3 seconds, respectively (Fig. 5a). For TLR4, the average time in confined domain in the absence and presence of RAGE is 3.3 seconds and 3.0 seconds, respectively (Fig. 5a). The average radius of confinement for RAGE in

the absence and presence of TLR4 is 0.20 μm and 0.22 μm, respectively (Fig. 5b). The average radius of confinement for TLR4 in the absence and presence of RAGE is 0.22 μm (Fig. 5b). These data show that RAGE and TLR4 enter into similar-sized confined domains and spend similar amounts of time in these confined domains before they diffuse out, regardless of whether the other receptor is expressed in the membrane. Finally, there is no change in the diffusion coefficient within confined domains whether one or both receptors are expressed in the membrane (Fig. 6b). While the diffusion properties are the same for RAGE and TLR4 within the confined domains, it is not possible to conclude from the SPT data that the chemical nature of the confined domains that RAGE and TLR4 enter into are the same.

# Brownian diffusion properties of RAGE and TLR4 are altered in the presence of the other receptor

RAGE and TLR4 show significant differences in their Brownian diffusion coefficients in the presence and absence of the other receptor. The average Brownian diffusion coefficient of RAGE in the absence of TLR4 is  $0.057~\mu m^2/s$ , and in the presence of TLR4 it is  $0.080~\mu m^2/s$  (Fig. 6a). When RAGE exhibits Brownian diffusion, the diffusion coefficient is faster in the presence of TLR4 compared to the diffusion coefficient when TLR4 is absent. The average Brownian diffusion coefficient of TLR4 in the absence of RAGE is  $0.117~\mu m^2/s$ , and in the presence of RAGE it is  $0.079~\mu m^2/s$  (Fig. 6a). When TLR4 exhibits Brownian diffusion, the diffusion coefficient is slower in the presence of RAGE compared to the diffusion when RAGE is absent. Notably, in cells where both RAGE and TLR4 are present, their average diffusion coefficients are approximately the same  $(0.080~\mu m^2/s$  and  $0.079~\mu m^2/s$ , respectively) as is the range of diffusion coefficients  $(0.006~to~0.169~\mu m^2/s)$ .

Lipid diffusion properties were measured in cells that express only RAGE, only TLR4, and both RAGE and TLR4 to determine the effect of the receptors on lipid mobility. DiI was used as a fluorescent lipid mimetic. To ensure single molecules were tracked, the DiI concentration in the culture medium was 10 nM. The average Brownian diffusion coefficient of lipids in these cells is 0.055 μm²/s (RAGE and TLR4), 0.060 μm²/s (RAGE), and 0.057 μm²/s (TLR4), respectively (Fig. S1a). There was no statistical difference in the Brownian diffusion coefficients, diffusion coefficients inside confined regions (Fig. S1b), time inside confined domains (Fig. S2a), and radius of the confined domains (Fig. S2b) for the lipid probe in any of the data sets. These data show that

the presence and absence of RAGE and TLR4 do not alter the membrane's lipid mobility as measured by the lipid mimetic DiI.

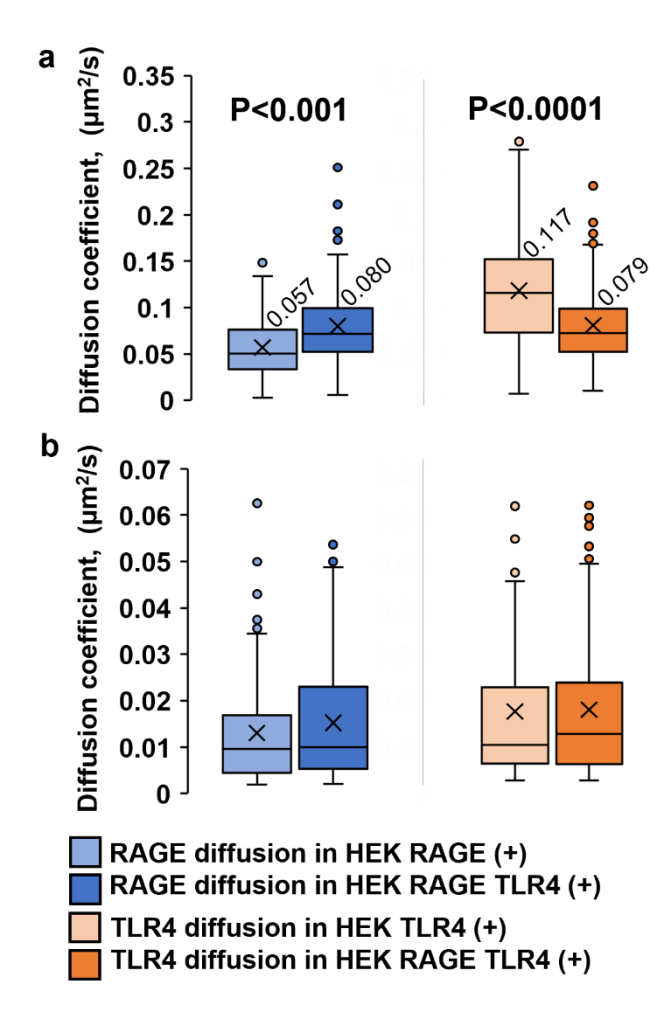


**Fig. 6** The box-and-whisker plots of the diffusion coefficients for (blue) RAGE and (orange) TLR4 trajectories. **a)** Brownian diffusion coefficients and **b)** diffusion coefficients inside the confined domains. The p-values below 0.05 show statistically significant differences between the cell line expressing only one receptor and the cell line expressing both receptors. When no p-value is listed, its value is above 0.05

The trajectories and diffusion properties discussed above were performed in separate cell populations (i.e., cell lines expressing only one receptor and a different cell line expressing both receptors). Two-color SPT utilized two spectrally separated QDs to simultaneously measure the diffusion properties of both receptors in the same cell line expressing both RAGE and TLR4.

During the simultaneous tracking, the total number of trajectories analyzed for RAGE and TLR4 were 1883 and 2001, respectively. The total trajectory time for RAGE was 386.2 minutes, and for TLR4 was 320 minutes. During this long observation time, RAGE and TLR4 were measured within 30 nanometers of each other only three times, with separation distances of 22 nm, 23 nm, and 30 nm (Fig. 7). It is important to note that the SPT experiments require a very low number of the receptors to be labeled with the QD to extract their position accurately. RAGE and TLR4 were expected to be spatially close many more than three times during the observation time, but SPT only captures a small number of these events due to the low number of receptors that are labeled. In the two-color SPT experiment, 22 nm was the closest distance between the QDs used to label the receptors. The size of the QDs is 15-20 nm (i.e., there is size polydispersity in the QDs). That means the closest distance that could be observed between the centers of two QDs would be 15-20 nm.

For all three events when RAGE and TLR4 were within less than 30 nm of each other, both receptors exhibited Brownian diffusion. No confined regions were measured when the receptors were spatially close to each other. The instantaneous diffusion coefficient at each time point of the trajectory was calculated by averaging the mean squared displacement of 10 preceding time points. In Fig. 7a, at 1.80 seconds, both QDs were 23 nm apart, and at 1.84 seconds (i.e., the next frame of the movie) they were 112 nm apart. Between 1.80 and 1.84 seconds, the instantaneous diffusion coefficient of RAGE changed from 0.091 µm<sup>2</sup>/s to 0.156 µm<sup>2</sup>/s and the diffusion coefficient of TLR4 remained the same (0.047  $\mu$ m<sup>2</sup>/s to 0.046  $\mu$ m<sup>2</sup>/s). During this time, RAGE diffusion is faster while TLR4 diffusion is slower compared to their average Brownian diffusion coefficients in HEK RAGE TLR4 (+) cells (Fig. 6a). In the same trajectory, two frames later at 1.92 seconds, both QDs were 22 nm apart and at 1.96 seconds they were 55 nm apart. The diffusion coefficient of RAGE was 0.212 µm<sup>2</sup>/s and 0.238 µm<sup>2</sup>/s at these times, and the diffusion coefficient of TLR4 remained approximately the same  $(0.070 \, \mu \text{m}^2/\text{s})$  and  $0.066 \, \mu \text{m}^2/\text{s}$ . The third time the QDs were less than 30 nm away from each other was measured in a different set of trajectories (Fig. 7b). At 8.48 seconds, both QDs were 30 nm apart. Between 8.48 and 8.52 seconds, the diffusion coefficient of RAGE was 0.017 μm<sup>2</sup>/s and 0.023 μm<sup>2</sup>/s, while the diffusion coefficient of TLR4 was 0.008 μm<sup>2</sup>/s and 0.007 µm<sup>2</sup>/s. Due to the low number of observations when the two receptors are less than 30 nm apart and the significant variability in the instantaneous diffusion coefficient throughout the trajectories, the statistical significance of these observations cannot be determined at this time. In

contrast to the number of events when the receptors are less than 30 nm apart, there are numerous times and trajectories when the two receptors are farther apart. Pearson correlation coefficients were calculated from the instantaneous diffusion coefficients of RAGE and TLR4 at each time point across their entire trajectories. 30 sets of trajectories were analyzed, and no strong correlation (-0.3 to +0.3) was found. Four representative sets of trajectories when the receptors are far apart are shown in Fig. S3.

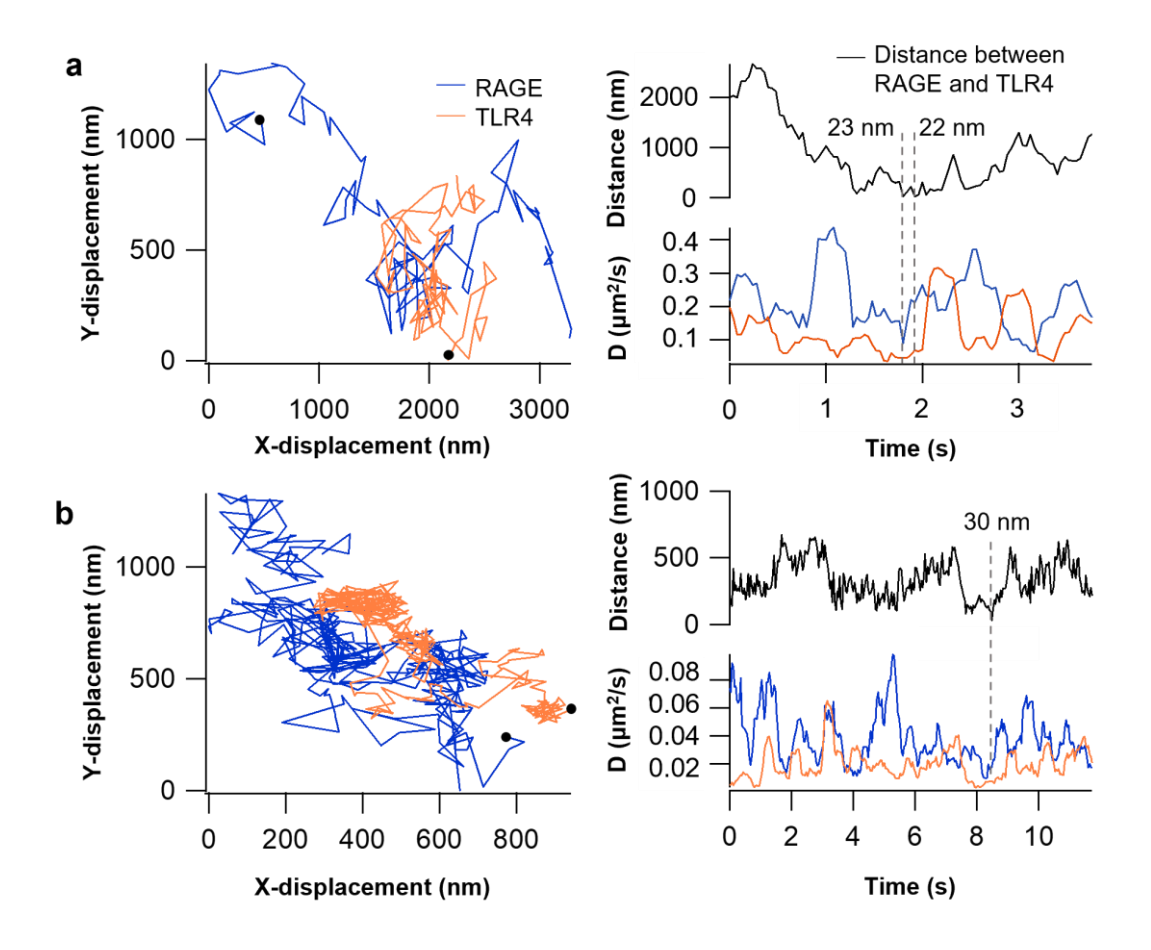


**Fig. 7** Two-color simultaneous single particle tracking of (blue) RAGE and (orange) TLR4 in the same HEK RAGE TLR4 (+) cell. The **two** sets of trajectories (a and b) represent the only times across all the data when RAGE and TLR4 are less than 30 nm apart. Left side graphs of **a** and **b** show the trajectories of (blue) RAGE and (orange) TLR4. Note: the starting time of each trajectory is shown as a solid black circle. The graphs on the right of **a** and **b** show (black) the relative distances between RAGE and TLR4 to see when the receptors are close in space and time and the instantaneous diffusion coefficients of (blue) RAGE and (orange) TLR4

The change in Brownian diffusion properties of RAGE or TLR4 in the presence of the other receptor is not the result of changes to lipid diffusion (membrane fluidity), and there is no evidence the diffusion is altered by the formation of stable RAGE/TLR4 clusters (two-color SPT experiments). It is known from the literature that RAGE can exist as monomers and oligomers on the cell membrane (Fritz, 2011). The binding of ligands promotes the formation of RAGE oligomerization, and interaction between the RAGE cytoplasmic tail and the Diaphanous-1 cytoplasmic protein changes the nanoscale clustering of RAGE (Zhu & Smith, 2019b). Before binding to ligand, the TLR4/MD-2 protein complex predominates in monomeric forms. Possible explanations for measured changes in Brownian diffusion properties in the absence of ligand are: altered interactions with cytoplasmic proteins in the presence of the other receptor, or alterations of RAGE/RAGE or TLR4/TLR4 clusters in the presence of the other receptor. The latter cannot be measured by SPT.

### **Conclusion**

Combining all the data, the following conclusions can be made. RAGE goes into *confined domains* more often than TLR4 but stays within domains of the same size for the same amount of time as TLR4, and this is independent of the presence of TLR4. The receptor's diffusion coefficients inside these confined domains are not affected by the presence of the other receptor. RAGE and TLR4 may go into domains with different chemical and physical properties, or they may go into the same domains. In either case, the diffusion properties of RAGE and TLR4 within the confined domains are not affected by the presence of the other receptor. Confined domains are important for RAGE and TLR4 receptors to initiate intracellular signaling in response to many ligands (Yan et al., 2023). RAGE and TLR4 share common ligands (e.g., advanced glycation endproducts, high mobility group box 1 protein, lipopolysaccharide), share common adaptor proteins (e.g., TIRAP and MyD88), and activate similar downstream signaling pathways (e.g., mitogen-activated protein kinases, extracellular signal-regulated kinase) within the cell (Gasiorowski et al., 2018; Hreggvidsdóttir et al., 2012; Prantner et al., 2020; Ramya et al., 2021; Sakaguchi et al., 2011; Yan et al., 2023; Zhong et al., 2020). A change in the RAGE and TLR4 diffusion properties inside confined domains may occur in cells exposed to ligand (Syed et al., 2016; Triantafilou et al., 2004), but as report herein for the absence of ligand, diffusion within confined domains remains unaffected by the presence of the other receptor.

The average Brownian diffusion properties of one receptor are affected by the presence of the other receptor, but the effect is not the same for both receptors. When both receptors are present in the cell membrane but tracked consecutively, they have a similar average diffusion coefficient. Both receptors were also tracked simultaneously. When both proteins came close to each other (i.e., the QDs were measured to be 30 nm apart), both RAGE and TLR4 diffusion coefficients were simultaneously slower or faster than their average diffusion coefficients. This suggests that the Brownian diffusion of these two receptors is correlated when the receptors are close together, however, the statistical significance of this observation is not known due to the limitations of the SPT technique. In all instances when the receptors were close, they remained close for only a short time (~40 ms, or the data collection rate). This suggests when the receptors are moving via Brownian diffusion close to each other, they are not forming stable clusters, or the clusters are very dynamic. Furthermore, while simultaneously tracking the receptors, there were no instances when both receptors were found within the same confined domain (i.e., exhibiting non-Brownian diffusion). Finally, the expression of the receptors was not associated with a change in lipid diffusion, suggesting that differences in the receptor's diffusion properties measured in the presence and absence of each other are via a mechanism that is specific to the receptors.

## Acknowledgments

This work was supported by the National Science Foundation under Grant Number CHE-2003308. The authors thank Dr. Chamari Wijesoorya for her initial direction and support in this project.

## **Author contributions**

**Sharifur Rahman:** Conceptualization, Methodology, Formal analysis, Investigation, Visualization, Writing-Original draft. **Mohammad Khalid Ibne Walid:** Conceptualization, Methodology, Formal analysis, Investigation, Visualization, Writing-Original draft. **Emily A. Smith:** Conceptualization, Methodology, Supervision, Writing-Review & Editing.

## Data availability

Data is available upon request.

#### **Declarations**

### **Conflict of interest statement**

The authors declare that they have no conflict of interest.

## Disclaimer

Any opinions, findings, conclusions, or recommendations expressed in this material are those of the authors and do not necessarily reflect the views of the National Science Foundation.

#### References

- Areal, H., Abrantes, J., & Esteves, P. J. (2011). Signatures of positive selection in Toll-like receptor (TLR) genes in mammals. *BMC Evolutionary Biology*, *11*, 368. https://doi.org/10.1186/1471-2148-11-368
- Bian, J. M., Wu, N., Su, R. Bin, & Li, J. (2012). Opioid receptor trafficking and signaling: What happens after opioid receptor activation? *Cellular and Molecular Neurobiology*, *32*(2), 167–184. https://doi.org/10.1007/s10571-011-9755-5
- Casula, M., Iyer, A. M., Spliet, W. G. M., Anink, J. J., Steentjes, K., Sta, M., Troost, D., & Aronica, E. (2011). Toll-like receptor signaling in amyotrophic lateral sclerosis spinal cord tissue. *Neuroscience*, *179*, 233–243. https://doi.org/10.1016/j.neuroscience.2011.02.001
- Chen, T., Huang, W., Qian, J., Luo, W., Shan, P., Cai, Y., Lin, K., Wu, G., & Liang, G. (2020). Macrophage-derived myeloid differentiation protein 2 plays an essential role in ox-LDL-induced inflammation and atherosclerosis. *EBioMedicine*, *53*. https://doi.org/10.1016/j.ebiom.2020.102706
- Fritz, G. (2011). RAGE: A single receptor fits multiple ligands. In *Trends in Biochemical Sciences* (Vol. 36, Issue 12, pp. 625–632). https://doi.org/10.1016/j.tibs.2011.08.008
- Gambin, Y., Lopez-Esparza, R., Reffay, M., Sierecki, E., Gov, N. S., Genest, M., Hodges, R. S., & Urbach, W. (2006). Lateral mobility of proteins in liquid membranes revisited.
  Proceedings of the National Academy of Sciences of the United States of America, 103(7), 2098–2102. https://doi.org/10.1073/pnas.0511026103
- Gąsiorowski, K., Brokos, B., Echeverria, V., Barreto, G. E., & Leszek, J. (2018). RAGE-TLR Crosstalk Sustains Chronic Inflammation in Neurodegeneration. *Molecular Neurobiology*, 55(2), 1463–1476. https://doi.org/10.1007/s12035-017-0419-4
- Goldin, A., Beckman, J. A., Schmidt, A. M., & Creager, M. A. (2006a). Advanced glycation end products: Sparking the development of diabetic vascular injury. In *Circulation* (Vol. 114, Issue 6, pp. 597–605). https://doi.org/10.1161/CIRCULATIONAHA.106.621854
- Goldin, A., Beckman, J. A., Schmidt, A. M., & Creager, M. A. (2006b). Advanced glycation end products: Sparking the development of diabetic vascular injury. *Circulation*, 114(6), 597–

- 605. https://doi.org/10.1161/CIRCULATIONAHA.106.621854
- Hreggvidsdóttir, H. S., Lundberg, A. M., Aveberger, A. C., Klevenvall, L., Andersson, U., & Harris, H. E. (2012). High mobility group box protein 1 (HMGB1)-partner molecule complexes enhance cytokine production by signaling through the partner molecule receptor. Molecular Medicine, 18(2), 224–230. https://doi.org/10.2119/molmed.2011.00327
- Ibrahim, Z. A., Armour, C. L., Phipps, S., & Sukkar, M. B. (2013). RAGE and TLRs: Relatives, friends or neighbours? *Molecular Immunology*, *56*(4), 739–744. https://doi.org/10.1016/j.molimm.2013.07.008
- Kim, S., Young Kim, S., Pribis, J. P., Lotze, M., Mollen, K. P., Shapiro, R., Loughran, P., Scott, M. J., & Billiar, T. R. (2013). Signaling of high mobility group box 1 (HMGB1) through toll-like receptor 4 in macrophages requires CD14. *Molecular Medicine*, 19(1), 88–98. https://doi.org/10.2119/molmed.2012.00306
- Lazar, A. M., Irannejad, R., Baldwin, T. A., Sundaram, A. B., Gutkind, J. S., Inoue, A., Dessauer, C. W., & Zastrow, M. Von. (2020). G protein-regulated endocytic trafficking of adenylyl cyclase type 9. *ELife*, 9, 1–24. https://doi.org/10.7554/eLife.58039
- Lin, L. (2006). RAGE on the Toll Road? Cellular & Molecular Immunology, 3(5), 351–358.
- Lin, L., Maingret, F., Groc, L., Rouiller, V., Clarke, S., Changjiang, Y., Pinaud, F., Gouzer, G., Schaible, D., Marchi-Artzner, V., Piehler, J., Dahan, M., Maynard, S. A., Triller, A., Ibrahim, Z. A., Armour, C. L., Phipps, S., Sukkar, M. B., Gasiorowski, K., ... Huh, N. ho. (2006). TIRAP, an adaptor protein for TLR2/4, transduces a signal from RAGE phosphorylated upon ligand binding. *International Journal of Molecular Sciences*, 55(5), 739–744. https://doi.org/10.1007/s12035-017-0419-4
- Mainali, D., & Smith, E. A. (2013a). Select cytoplasmic and membrane proteins increase the percentage of immobile integrins but do not affect the average diffusion coefficient of mobile integrins. *Analytical and Bioanalytical Chemistry*, 405(26), 8561–8568. https://doi.org/10.1007/s00216-013-7279-1
- Mainali, D., & Smith, E. A. (2013b). The effect of ligand affinity on integrins' lateral diffusion in cultured cells. *European Biophysics Journal*, 42(4), 281–290.

- https://doi.org/10.1007/s00249-012-0873-x
- Manzoni, M., Monti, E., Bresciani, R., Bozzato, A., Barlati, S., Bassi, M. T., & Borsani, G. (2004). Overexpression of wild-type and mutant mucolipin proteins in mammalian cells: Effects on the late endocytic compartment organization. *FEBS Letters*, *567*(2–3), 219–224. https://doi.org/10.1016/j.febslet.2004.04.080
- Maynard, S. A., & Triller, A. (2019). Inhibitory Receptor Diffusion Dynamics. *Frontiers in Molecular Neuroscience*, 12(December), 1–9. https://doi.org/10.3389/fnmol.2019.00313
- McGettrick, A. F., & O'Neill, L. A. J. (2007). Toll-like receptors: Key activators of leucocytes and regulator of haematopoiesis. In *British Journal of Haematology* (Vol. 139, Issue 2, pp. 185–193). https://doi.org/10.1111/j.1365-2141.2007.06802.x
- Menchón, S. A., Martín, M. G., & Dotti, C. G. (2012). APM\_GUI: Analyzing particle movement on the cell membrane and determining confinement. *BMC Biophysics*, *5*(1). https://doi.org/10.1186/2046-1682-5-4
- Michalet, X., Pinaud, F. F., Bentolila, L. A., Tsay, J. M., Doose, S., Li, J. J., Sundaresan, G., Wu, A. M., Gambhir, S. S., & Weiss, S. (2005). *Quantum Dots for Live Cells, in Vivo Imaging, and Diagnostics*. www.sciencemag.org/cgi/content/full/307/5709/538/DC1,
- Nozeret, K., Boucharlat, A., Agou, F., & Buddelmeijer, N. (2019). A sensitive fluorescence-based assay to monitor enzymatic activity of the essential integral membrane protein Apolipoprotein N-acyltransferase (Lnt). *Scientific Reports*, 9(1), 25–28. https://doi.org/10.1038/s41598-019-52106-8
- Płóciennikowska, A., Hromada-Judycka, A., Borzęcka, K., & Kwiatkowska, K. (2015). Cooperation of TLR4 and raft proteins in LPS-induced pro-inflammatory signaling. *Cellular and Molecular Life Sciences*, 72(3), 557–581. https://doi.org/10.1007/s00018-014-1762-5
- Prantner, D., Nallar, S., & Vogel, S. N. (2020). The role of RAGE in host pathology and crosstalk between RAGE and TLR4 in innate immune signal transduction pathways. *FASEB Journal*, *34*(12), 15659–15674. https://doi.org/10.1096/fj.202002136R
- Ramya, R., Coral, K., & Bharathidevi, S. R. (2021). RAGE silencing deters CML-AGE induced inflammation and TLR4 expression in endothelial cells. *Experimental Eye Research*,

- 206(November 2020). https://doi.org/10.1016/j.exer.2021.108519
- Rouiller, V., Clarke, S., Changjiang, Y., Pinaud, F., Gouzer, G., Schaible, D., Marchi-Artzner, V., Piehler, J., & Dahan, M. (2009). High-affinity labeling and tracking of individual histidine-tagged proteins in live cells using Ni2+ tris-nitrilotriacetic acid quantum dot conjugates. *Nano Letters*, *9*(3), 1228–1234. https://doi.org/10.1021/nl9001298
- Sakaguchi, M., Murata, H., Yamamoto, K. ichi, Ono, T., Sakaguchi, Y., Motoyama, A., Hibino, T., Kataoka, K., & Huh, N. ho. (2011). TIRAP, an adaptor protein for TLR2/4, transduces a signal from RAGE phosphorylated upon ligand binding. *PLoS ONE*, *6*(8). https://doi.org/10.1371/journal.pone.0023132
- Sbalzarini, I. F., & Koumoutsakos, P. (2005). Feature point tracking and trajectory analysis for video imaging in cell biology. *Journal of Structural Biology*, *151*(2), 182–195. https://doi.org/10.1016/j.jsb.2005.06.002
- Schopf, K., & Huber, A. (2017). Membrane protein trafficking in Drosophila photoreceptor cells. *European Journal of Cell Biology*, 96(5), 391–401.

  https://doi.org/10.1016/j.ejcb.2016.11.002
- Semini, G., Paape, D., Paterou, A., Schroeder, J., Barrios-Llerena, M., & Aebischer, T. (2017). Changes to cholesterol trafficking in macrophages by Leishmania parasites infection. *MicrobiologyOpen*, 6(4), 1–13. https://doi.org/10.1002/mbo3.469
- Simson, R., Sheets, E. D., & Jacobson, K. (1995). Detection of temporary lateral confinement of membrane proteins using single-particle tracking analysis. *Biophysical Journal*, 69(3), 989–993. https://doi.org/10.1016/S0006-3495(95)79972-6
- Syed, A., Zhu, Q., & Smith, E. A. (2016). Ligand binding affinity and changes in the lateral diffusion of receptor for advanced glycation endproducts (RAGE). *Biochimica et Biophysica Acta Biomembranes*, *1858*(12), 3141–3149. https://doi.org/10.1016/j.bbamem.2016.10.001
- Syed, A., Zhu, Q., & Smith, E. A. (2018). Lateral diffusion and signaling of receptor for advanced glycation end-products (RAGE): a receptor involved in chronic inflammation. *European Biophysics Journal*, 47(1), 39–48. https://doi.org/10.1007/s00249-017-1227-5

- Triantafilou, M., Morath, S., Mackie, A., Hartung, T., & Triantafilou, K. (2004). Lateral diffusion of Toll-like receptors reveals that they are transiently confined within lipid rafts on the plasma membrane. *Journal of Cell Science*, 117(17), 4007–4014. https://doi.org/10.1242/jcs.01270
- Trofimov, Y. A., Krylov, N. A., & Efremov, R. G. (2019). Confined dynamics of water in transmembrane pore of trpv1 ion channel. *International Journal of Molecular Sciences*, 20(17), 1–13. https://doi.org/10.3390/ijms20174285
- Van Beijnum, J. R., Buurman, W. A., & Griffioen, A. W. (2008). Convergence and amplification of toll-like receptor (TLR) and receptor for advanced glycation end products (RAGE) signaling pathways via high mobility group B1 (HMGB1). *Angiogenesis*, 11(1), 91–99. https://doi.org/10.1007/s10456-008-9093-5
- Wang, H., Lee, E. W., Cai, X., Ni, Z., Zhou, L., & Mao, Q. (2008). Membrane topology of the human breast cancer resistance protein (BCRP/ABCG2) determined by epitope insertion and immunofluorescence. *Biochemistry*, 47(52), 13778–13787. https://doi.org/10.1021/bi801644v
- Xie, J., Reverdatto, S., Frolov, A., Hoffmann, R., Burz, D. S., & Shekhtman, A. (2008). Structural basis for pattern recognition by the receptor for advanced glycation end products (RAGE). *Journal of Biological Chemistry*, 283(40), 27255–27269. https://doi.org/10.1074/jbc.M801622200
- Yan, L., Li, Y., Tan, T., Qi, J., Fang, J., Guo, H., Ren, Z., Gou, L., Geng, Y., Cui, H., Shen, L., Yu, S., Wang, Z., & Zuo, Z. (2023). RAGE–TLR4 Crosstalk Is the Key Mechanism by Which High Glucose Enhances the Lipopolysaccharide-Induced Inflammatory Response in Primary Bovine Alveolar Macrophages. *International Journal of Molecular Sciences*, 24(8). https://doi.org/10.3390/ijms24087007
- Zeuner, M. T., Krüger, C. L., Volk, K., Bieback, K., Cottrell, G. S., Heilemann, M., & Widera,
  D. (2016). Biased signalling is an essential feature of TLR4 in glioma cells. *Biochimica et Biophysica Acta Molecular Cell Research*, 1863(12), 3084–3095.
  https://doi.org/10.1016/j.bbamcr.2016.09.016

- Zhong, H., Li, X., Zhou, S., Jiang, P., Liu, X., Ouyang, M., Nie, Y., Chen, X., Zhang, L., Liu, Y., Tao, T., & Tang, J. (2020). Interplay between RAGE and TLR4 Regulates HMGB1-Induced Inflammation by Promoting Cell Surface Expression of RAGE and TLR4. *The Journal of Immunology*, 205(3), 767–775. https://doi.org/10.4049/jimmunol.1900860
- Zhu, Q., & Smith, E. A. (2019a). Diaphanous-1 affects the nanoscale clustering and lateral diffusion of receptor for advanced glycation endproducts (RAGE). In *Biochimica et Biophysica Acta Biomembranes* (Vol. 1861, Issue 1, pp. 43–49). https://doi.org/10.1016/j.bbamem.2018.10.015
- Zhu, Q., & Smith, E. A. (2019b). Diaphanous-1 affects the nanoscale clustering and lateral diffusion of receptor for advanced glycation endproducts (RAGE). *Biochimica et Biophysica Acta Biomembranes*, *1861*(1), 43–49. https://doi.org/10.1016/j.bbamem.2018.10.015